

Relative Entropy of Random States and Black Holes

Jonah Kudler-Flam^{1,*}

¹*Kadanoff Center for Theoretical Physics, University of Chicago, Chicago, IL 60637, USA*

(Dated: December 23, 2024)

We study the subsystem relative entropy of highly excited quantum states. First, we independently draw the two density matrices from the Wishart ensemble and develop a large- N diagrammatic technique to compute the relative entropy. The solution is monotonically increasing from zero and exactly expressed in terms of hypergeometric functions. We compare the analytic results to small- N numerics, finding precise agreement. We then apply this formalism to “fixed-area” states in the AdS/CFT correspondence. In this context, the relative entropy measures the distinguishability between different black hole microstates. We find that black hole microstates are distinguishable even when the observer has arbitrarily small access to the boundary region, though the distinguishability is nonperturbatively small in Newton’s constant. Finally, we interpret these results in the context of the subsystem Eigenstate Thermalization Hypothesis (ETH), concluding that holographic systems obey subsystem ETH up to subsystems half the size of the total system.

Introduction. Random matrices are a unifying subject in quantum physics. From encoding quantum information [1], to characterizing complicated many-body systems and quantum chaos [2], to serving as toy models of the black hole information problem [3, 4], random quantum states have become invaluable across many distinct subfields. Moreover, the mathematical field of random matrix theory is very mature, enabling analytical calculations in random states that would be otherwise intractable.

With these general motivations in mind, we study the relative entropy of random quantum states. The relative entropy between two density matrices ρ and σ is defined as

$$D(\rho||\sigma) = \text{Tr} [\rho (\log \rho - \log \sigma)]. \quad (1)$$

As a distinguishability measure, it obeys various nice properties, such as positivity with $D(\rho||\sigma) = 0$ if and only if $\rho = \sigma$. Crucially, the relative entropy is monotonic under quantum operations [5]

$$D(\mathcal{N}(\rho)||\mathcal{N}(\sigma)) \leq D(\rho||\sigma), \quad (2)$$

where \mathcal{N} is any completely-positive trace-preserving map. A particularly important quantum channel that we will come back to is the partial trace operation. Monotonicity here means that density matrices become less distinguishable as you throw out more information about them, an intuitive notion.

Relative entropy is truly the mother of all quantities in quantum information theory. While at face value, it just measures the distinguishability between two density matrices, upon further inspection, its fundamental properties underlie many of the deepest universal statements about quantum mechanics [6, 7], quantum field theory [8–10], and quantum gravity [11, 12].

We first introduce random mixed states and their diagrammatic representation. We then embark on our main computation of the relative entropy between independently sampled random density matrices, finding a closed form solution in terms of hypergeometric functions. The general formula is exact in the limit of large Hilbert space dimensions but we find it to be remarkably accurate even for small Hilbert space dimensions. Afterwards, we apply our formalism to the AdS/CFT correspondence. Our central conclusion in this analysis is that the relative entropy between black hole microstates is finite, though non-perturbatively small in Newton’s constant up until the subsystem is half of the total system size. This is an extremely strong version of the eigenstate thermalization hypothesis [13, 14], a statement that we subsequently make precise. We wrap up with speculations regarding future directions and the general applicability of our results to chaotic quantum systems.

Random Mixed States. We begin with a Haar random pure state on a bipartite Hilbert space $\mathcal{H}_A \otimes \mathcal{H}_B$

$$|\Psi\rangle = \sum_{i=1}^{d_A} \sum_{\alpha=1}^{d_B} X_{i\alpha} |i\rangle_A \otimes |\alpha\rangle_B, \quad (3)$$

where the states in the sum are orthonormal bases for the sub-Hilbert spaces of dimensions d_A and d_B . The $X_{i\alpha}$ ’s are independently distributed complex Gaussian random variables with joint probability distribution

$$P(\{X_{i\alpha}\}) = \mathcal{Z}^{-1} \exp [-d_A d_B \text{Tr} (XX^\dagger)], \quad (4)$$

where \mathcal{Z} is the normalization constant, ensuring the expression defines a probability. The random induced states on \mathcal{H}_A are then

$$\rho_A = \frac{XX^\dagger}{\text{Tr}(XX^\dagger)}. \quad (5)$$

We note that the denominator is a random variable that is sharply peaked around unity, so we can ignore it in the limit of large Hilbert space dimension [15]

$$\rho_A \simeq XX^\dagger. \quad (6)$$

* jkudlerflam@uchicago.edu

This defines the Wishart ensemble. We now introduce a diagrammatic representation of the density matrix [16–18]

$$[\langle \Psi \rangle \langle \Psi \rangle]_{i\alpha, j\beta} = X_{i\alpha}^* X_{j\beta} = \begin{array}{c} i\alpha \quad \beta j \\ | \quad | \end{array} . \quad (7)$$

The solid and dashed lines correspond to subsystems A and B respectively. Matrix manipulations are done at the bottom edge of the diagram. For example, the partial trace over \mathcal{H}_B is

$$[\rho_A]_{i,j} = \sum_{\alpha=1}^{d_B} X_{i\alpha}^* X_{j\alpha} \equiv \begin{array}{c} i\alpha \quad \alpha j \\ | \quad | \end{array} . \quad (8)$$

Ensemble averaging is done at the top of the diagram with propagators carrying weight

$$\begin{array}{c} \text{---} \\ \text{---} \end{array} \equiv \langle X_{i\alpha}^* X_{j\beta} \rangle = \frac{1}{d_A d_B} \delta_{ij} \delta_{\alpha\beta}. \quad (9)$$

Putting these operations together, we can, for example, take the trace of the density matrix

$$\langle \text{Tr} \rho_A \rangle = \begin{array}{c} \text{---} \\ \text{---} \end{array} = 1, \quad (10)$$

where every closed loop gives a factor of the Hilbert space dimension. The diagrammatic rules for averaging assert that we must sum over all possible contractions of the bras and kets. For relative entropy, we need two independent density matrices, ρ_A and σ_A . These must be averaged over the ensemble separately. To make this distinction, we color σ_A red.

The logarithms in the definition of relative entropy make the quantity significantly more difficult to compute analytically than simple powers of the density matrices. Happily, a replica trick for the relative entropy has been developed that re-expresses the logarithm as a limit of appropriate powers [19]

$$D(\rho || \sigma) = \lim_{n \rightarrow 1} \frac{1}{n-1} (\log \text{Tr} \rho^n - \log \text{Tr} \rho \sigma^{n-1}). \quad (11)$$

We will compute these two terms separately. The first term is recognized as minus the Rényi entropy. For $n = 2$, we have

$$\text{Tr} \rho_A^2 = \begin{array}{c} \text{---} \\ \text{---} \end{array} \quad (12)$$

The ensemble average is a sum of the two contractions

$$\langle \text{Tr} \rho_A^2 \rangle = \begin{array}{c} \text{---} \\ \text{---} \end{array} + \begin{array}{c} \text{---} \\ \text{---} \end{array}, \quad (13)$$

immediately giving $d_A^{-1} + d_B^{-1}$. This can be generalized to arbitrary powers. Because of the sum over all possible

contractions, in general, the moments are expressible as a sum over the permutation group

$$\langle \text{Tr} \rho_A^n \rangle = \frac{1}{(d_A d_B)^n} \sum_{\tau \in S_n} d_A^{D(\eta^{-1} \circ \tau)} d_B^{D(\tau)}, \quad (14)$$

where $D(\cdot)$ is the number of cycles in the permutation and η is the cyclic permutation. When the Hilbert spaces are large, only the terms that maximize $D(\eta^{-1} \circ \tau) + D(\tau)$ will contribute to the sum at leading order. These are known as the non-crossing permutations and have $D(\eta^{-1} \circ \tau) + D(\tau) = n + 1$. Much is known about this special subset of permutations including that the number of such permutations with $D(\eta^{-1} \circ \tau) = k$ is given by the Narayana number

$$N_{n,k} = \frac{1}{n} \binom{n}{k} \binom{n}{k-1}. \quad (15)$$

Thus, the sum becomes

$$\begin{aligned} \langle \text{Tr} \rho_A^n \rangle &= \frac{1}{(d_A d_B)^n} \sum_{k=1}^n N_{n,k} d_A^k d_B^{n+1-k} \\ &= d_A^{1-n} {}_2F_1 \left(1-n, -n; 2; \frac{d_A}{d_B} \right), \end{aligned} \quad (16)$$

where ${}_2F_1$ is a hypergeometric function. This reproduces Page's famous result [20].

Next, we consider the second term of (11). For simplicity, we first consider the overlap between the two density matrices which, as a diagram, looks like

$$\text{Tr}(\rho_A \sigma_A) = \begin{array}{c} \text{---} \\ \text{---} \end{array} \quad (17)$$

We must ensemble average the black and red lines separately, so there is only a single term

$$\langle \text{Tr}(\rho_A \sigma_A) \rangle = \begin{array}{c} \text{---} \\ \text{---} \end{array}, \quad (18)$$

giving d_A^{-1} . We again generalize this to arbitrary powers by expressing the moments in terms of a sum over the permutation group

$$\langle \text{Tr}(\rho_A \sigma_A^{n-1}) \rangle = \frac{1}{(d_A d_B)^n} \sum_{\tau \in \mathbb{I} \times S_{n-1}} d_A^{D(\eta^{-1} \circ \tau)} d_B^{D(\tau)}. \quad (19)$$

The crucial difference between this expression and (14) is that the sum is only over a subgroup of permutations, namely the ones that stabilize the first element. These permutations still contain many non-crossing permutations that will dominate the sum.

The combinatorics of these non-crossing permutations are encoded within the beautiful formula of Kreweras which states that the number of non-crossing permutations of type $(1^{m_1} 2^{m_2} \dots n^{m_n})$ is [21, 22]

$$\#NC_n\{m_i\} = \frac{n(n-1)\dots(n-b+2)}{m_1!m_2!\dots m_n!}, \quad (20)$$

where $b \equiv \sum_i m_i \geq 2$. We are able to deduce that the sum of non-crossing permutations can be reorganized as

$$\begin{aligned} \langle \text{Tr} \rho_A \sigma_A^{n-1} \rangle &= \frac{1}{(d_A d_B)^n} \sum_{k=1}^{n-1} C_{n,k} d_A^k d_B^{n+1-k}, \\ C_{n,k} &\equiv \frac{1}{n-k} \binom{n-1}{k} \binom{n-2}{k-1}. \end{aligned} \quad (21)$$

Like the Rényi entropies, this may also be written as a hypergeometric function

$$\langle \text{Tr} \rho_A \sigma_A^{n-1} \rangle = d_A^{1-n} {}_2F_1 \left(1-n, 2-n; 2; \frac{d_A}{d_B} \right). \quad (22)$$

Combining (16) and (22), we can unambiguously take the $n \rightarrow 1$ limit to find the relative entropy¹

$$\begin{aligned} D(\rho_A \parallel \sigma_A) &= - {}_2F_1^{(0,1,0,0)} \left(-1, 0, 2, \frac{d_A}{d_B} \right) \\ &+ {}_2F_1^{(0,1,0,0)} \left(1, 0, 2, \frac{d_A}{d_B} \right) - {}_2F_1^{(1,0,0,0)} \left(-1, 0, 2, \frac{d_A}{d_B} \right) \\ &+ {}_2F_1^{(1,0,0,0)} \left(1, 0, 2, \frac{d_A}{d_B} \right). \end{aligned} \quad (23)$$

This is our main result. The superscripts denote derivatives on the corresponding arguments. This formula is zero when $d_A/d_B \rightarrow 0$. This is to be expected because density matrices become indistinguishable when most of the information is “traced away.” The relative entropy monotonically increases with d_A/d_B , reaching a curious value of $3/2$ when $d_A = d_B$. This monotonic behavior is just a restatement of the monotonicity of relative entropy under the partial trace quantum channel. For $d_A > d_B$, the density matrices are rank deficient leading to the formula giving a value with a small imaginary part asymptoting to $-\pi$. The real part of the function continues to monotonically increase, diverging linearly as $D(\rho_A \parallel \sigma_A) \rightarrow \frac{d_A}{2d_B}$. This suggests that this may still be a meaningful quantity, though we should really only trust the solution when it is real. We plot this function in Fig. 1 and compare to numerics, finding very good agreement even for the relatively small Hilbert space dimensions that are accessible on a classical computer.

Black Hole Microstates. Here, we reinterpret (23) in the context of the AdS/CFT correspondence. In this correspondence, high energy pure states in the boundary conformal field theory are dual to black holes microstates in the bulk. Relative entropy then tells us how well we can distinguish different black hole microstates of equal energy, a notoriously difficult task that, a priori, one would expect to require knowledge of the full ultraviolet complete quantum gravity theory, such as string

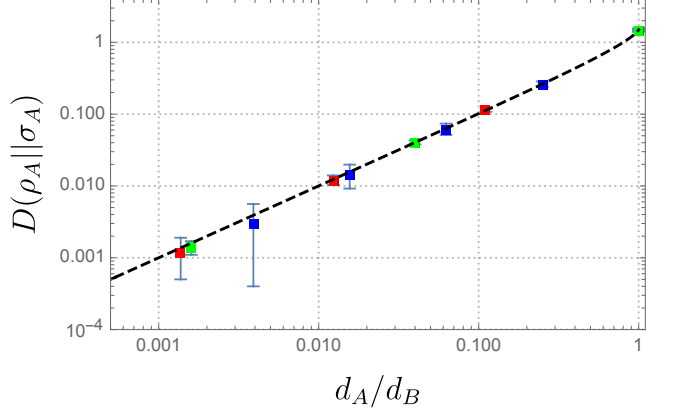


FIG. 1. Comparison of equation (23) (dashed line) with numerics. The blue, red, and green data points are for total Hilbert space sizes of 1024, 6561, and 15625 respectively. The fluctuations in the relative entropy are clearly suppressed as the dimension is increased, signaling self averaging.

theory [23]. Surprisingly, we show that this is actually possible just from semiclassical gravity, which is related to the recent surprise that the Page curve can be calculated from semiclassical gravity [24, 25].

This is simplest for “fixed-area states” [26, 27], which will be enough for our purposes. Fixed area states are holographic states where the areas of gauge-invariant surfaces in the bulk have been measured. These states have played an important role in the understanding of holographic entanglement entropy and quantum error correction.

While many details can be found in the original papers and illuminating follow-ups [28–32], we will only present what is necessary for our analysis. We consider states where two surfaces have been measured. These are the two candidate extremal surfaces, γ_1 and γ_2 , that compute the von Neumann entropy [33], depicted in Fig. 2. The two surfaces wrap the black hole horizon in topologically distinct manners. In the gravitational replica trick, the codimension-one region bounded by γ_1 and A is glued cyclically to the next replica, while the region between γ_2 and B is simply glued to the same replica. These gluings are determined by the asymptotic boundary conditions. The interesting region between γ_1 and γ_2 is not fixed by the boundary conditions and can therefore be glued using any permutation. This can be thought of as a sum over “replica wormholes” [32].

To compute the relative entropy between two different black hole microstates, we must compute

$$\text{Tr}(\rho_A \sigma_A^{n-1}) = \frac{\mathcal{Z}(\rho_A \sigma_A^{n-1})}{\mathcal{Z}(\rho_A) \mathcal{Z}(\sigma_A)^{n-1}}, \quad (24)$$

where \mathcal{Z} is the gravitational path integral evaluated on-shell with the boundary conditions dictated by the argument. Due to nice properties of fixed area states, the only contributions to the on-shell action (after normalization) come from the conical deficits that can occur at

¹ In general, the ensemble average and logarithm do not commute, requiring a further replica trick. However, these operations approximately commute for large Hilbert space dimensions.

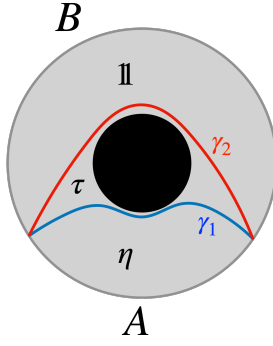


FIG. 2. Depicted is a black hole geometry with the boundary partitioned into regions A and B . There are two competing extremal surfaces, γ_1 and γ_2 , that we fix the area of. When performing the replica trick, we compute the path integral on n copies of this geometry. Each bulk region is labeled by the permutation element that governs how it is glued among the copies.

γ_1 and γ_2 , leading to

$$\text{Tr}(\rho_A \sigma_A^{n-1}) = \sum_{\tau \in \mathbb{1} \times S_{n-1}} \frac{e^{(D(\eta^{-1} \circ \tau) A_1 + D(\tau) A_2)/4G_N}}{e^{n(A_1 + A_2)/4G_N}}, \quad (25)$$

where A_1 and A_2 are the areas of the fixed surfaces and G_N is Newton's constant. This expression is identical to (19) once we identify $d_A = e^{A_1/4G_N}$ and $d_B = e^{A_2/4G_N}$. A similar conclusion is made for $\text{Tr}(\rho_A^n)$. Therefore, the relative entropy between black hole microstates is given by (23), which is UV finite because while the areas are themselves divergent, their difference is regulator independent. It is important to note that for small A_1 , i.e. small boundary subregion A , the relative entropy is nonzero, meaning the two black hole microstates are distinguishable! The catch is that the distinguishability is non-perturbatively small in Newton's constant, $O(e^{-1/G_N})$. However, as A_1 approaches A_2 , the relative entropy becomes $O(1)$. The transition from $O(e^{-1/G_N})$ to $O(1)$ occurs in an extremely tiny window when $(A_2 - A_1)/4G_N \lesssim \log 2$, roughly meaning that region A contains one less qubit of information than region B .

In passing, we note that these results also apply to the relative entropy of two states in the Jackiw-Teitelboim gravity plus end-of-the-world brane model of black hole evaporation from Ref. [32] in the case that the black hole is in the microcanonical ensemble.

Subsystem Eigenstate Thermalization. Subsystem ETH is a generalization of the standard local ETH story and is significantly stronger. While ETH is a statement about local operators, subsystem ETH is a statement that finite subregions appear thermal. Precisely, subsystem ETH holds when sufficiently highly excited eigenstates have reduced density matrices that are exponentially close in trace distance to some universal density

matrices, such as the microcanonical ensemble [34]

$$T(\rho_\psi, \rho_{univ}) \equiv |\rho_\psi - \rho_{univ}|_1 \leq O(e^{-S(E)/2}), \quad (26)$$

where $e^{S(E)}$ is the density of states of the full system. In the context of holography, the entropy scales as $O(G_N^{-1})$, so subsystem ETH just means that the trace distance is nonperturbatively small in Newton's constant.

We now invoke the quantum Pinsker inequality

$$D(\rho||\sigma) \geq \frac{1}{2} T(\rho, \sigma)^2. \quad (27)$$

We previously found $D(\rho_A||\sigma_A)$ to scale as $O(e^{-1/G_N})$ on average for any two black hole microstates with fixed area. This implies that the trace distance is, at most, $O(e^{-1/G_N})$. The trace distance defines a metric on the space of density matrices, so if a typical state is close to a measure one set of all other states, then the universal density matrix should sit within this ball. We therefore claim that fixed area states in all dimensions obey subsystem ETH for subsystems less than half the total system size. The violation of subsystem ETH only occurs when $(A_2 - A_1)/4G_N \lesssim \log 2$.

Discussion. There are various interesting directions that lie outside the scope of this paper: (i) We have computed the average relative entropy between typical random mixed states. However, we have not fixed the complete distribution. It would be interesting to characterize the fluctuations in relative entropy. The numerical results suggest that these are suppressed in the Hilbert space dimension. Higher moments of the relative entropy can be computed using the same technology we have developed in this paper. (ii) In our applications to holography, we focused on fixed-area states. More generic states are superpositions of fixed-area states with a sharply peaked Gaussian distributions of width $O(\sqrt{G_N})$ [29]. It is important to study the relative entropy of these more generic states to verify that the relative entropy is qualitatively the same. We can invoke convexity of the trace distance

$$T \left(\sum_i p_i \rho_i, \sum_i q_i \sigma_i \right) \leq T(p_i, q_i) + \sum_i p_i T(\rho_i, \sigma_i), \quad (28)$$

where the ρ_i and σ_i 's are fixed area states and $T(p_i, q_i)$ is the classical trace distance between probability distributions. We have already shown that the second term on the right hand side is $O(e^{-1/G_N})$. If we assume that the probability distributions are Gaussian with equal widths but centered at fixed areas a distance at most $O(e^{-1/G_N})$ apart i.e. within the same microcanonical window, then it is a straightforward exercise to confirm that the first term is also $O(e^{-1/G_N})$, confirming subsystem ETH. However, if the widths of the Gaussian distributions are different, even by an amount polynomial in G_N , the bound will no longer be tight. It would be fascinating if these corrections led to violations of eigenstate thermalization. (iii)

One of our motivations to study random states is that they should be representative of generic excited states in nonintegrable quantum systems. It is clearly interesting to look into how accurately our results characterize real Hamiltonian systems (beyond holography). We provide preliminary numerical results for the Sachdev-Ye-Kitaev (SYK) model and for spin chains in the supplemental material. While the SYK eigenstates mimic random matrix theory, we find that chaotic spin chain eigenstates have close to, but larger, relative entropy than random states and integrable eigenstates have even larger relative en-

tropy and much larger fluctuations. We hope to report a more systematic study in the future.

Acknowledgements. I am grateful to Chris Akers, Hong Liu, Pratik Rath, Shinsei Ryu, Hassan Shapourian, and Shreya Vardhan for helpful discussions and comments. I am supported through a Simons Investigator Award to Shinsei Ryu from the Simons Foundation (Award Number: 566166).

Note Added. After the completion of this work, I became aware of an independent project with overlapping results on the computation of relative entropy [35].

[1] B. Collins and I. Nechita, Random matrix techniques in quantum information theory, *Journal of Mathematical Physics* **57**, 015215 (2016), arXiv:1509.04689 [quant-ph].

[2] L. D’Alessio, Y. Kafri, A. Polkovnikov, and M. Rigol, From quantum chaos and eigenstate thermalization to statistical mechanics and thermodynamics, *Advances in Physics* **65**, 239 (2016), arXiv:1509.06411 [cond-mat.stat-mech].

[3] D. N. Page, Information in black hole radiation, *Phys. Rev. Lett.* **71**, 3743 (1993), arXiv:hep-th/9306083 [hep-th].

[4] P. Hayden and J. Preskill, Black holes as mirrors: quantum information in random subsystems, *Journal of High Energy Physics* **2007**, 120 (2007), arXiv:0708.4025 [hep-th].

[5] G. Lindblad, Completely positive maps and entropy inequalities, *Comm. Math. Phys.* **40**, 147 (1975).

[6] G. Lindblad, Expectations and entropy inequalities for finite quantum systems, *Comm. Math. Phys.* **39**, 111 (1974).

[7] V. Vedral, The role of relative entropy in quantum information theory, *Reviews of Modern Physics* **74**, 197 (2002), arXiv:quant-ph/0102094 [quant-ph].

[8] H. Casini and M. Huerta, A finite entanglement entropy and the c-theorem, *Physics Letters B* **600**, 142 (2004), arXiv:hep-th/0405111 [hep-th].

[9] T. Faulkner, R. G. Leigh, O. Parrikar, and H. Wang, Modular Hamiltonians for deformed half-spaces and the averaged null energy condition, *Journal of High Energy Physics* **2016**, 38 (2016), arXiv:1605.08072 [hep-th].

[10] S. Balakrishnan, T. Faulkner, Z. U. Khandker, and H. Wang, A general proof of the quantum null energy condition, *Journal of High Energy Physics* **2019**, 20 (2019), arXiv:1706.09432 [hep-th].

[11] H. Casini, Relative entropy and the Bekenstein bound, *Classical and Quantum Gravity* **25**, 205021 (2008), arXiv:0804.2182 [hep-th].

[12] A. C. Wall, Proof of the generalized second law for rapidly changing fields and arbitrary horizon slices, *Phys. Rev. D* **85**, 104049 (2012), arXiv:1105.3445 [gr-qc].

[13] J. M. Deutsch, Quantum statistical mechanics in a closed system, *Phys. Rev. A* **43**, 2046 (1991).

[14] M. Srednicki, Chaos and quantum thermalization, *Phys. Rev. E* **50**, 888 (1994), arXiv:cond-mat/9403051 [cond-mat].

[15] K. Zyczkowski and H.-J. Sommers, Induced measures in the space of mixed quantum states, *Journal of Physics A Mathematical General* **34**, 7111 (2001), arXiv:quant-ph/0012101 [quant-ph].

[16] E. Brézin and A. Zee, Universal relation between Green functions in random matrix theory, *Nuclear Physics B* **453**, 531 (1995), arXiv:cond-mat/9507032 [cond-mat].

[17] J. Jurkiewicz, G. Lukaszewski, and M. A. Nowak, Diagrammatic Approach to Fluctuations in the Wishart Ensemble, *Acta Physica Polonica B* **39**, 799 (2008).

[18] H. Shapourian, S. Liu, J. Kudler-Flam, and A. Vishwanath, Entanglement negativity spectrum of random mixed states: A diagrammatic approach, arXiv e-prints , arXiv:2011.01277 (2020), arXiv:2011.01277 [cond-mat.str-el].

[19] N. Lashkari, Modular Hamiltonian for Excited States in Conformal Field Theory, *Phys. Rev. Lett.* **117**, 041601 (2016), arXiv:1508.03506 [hep-th].

[20] D. N. Page, Average entropy of a subsystem, *Phys. Rev. Lett.* **71**, 1291 (1993), arXiv:gr-qc/9305007 [gr-qc].

[21] G. Kreweras, Sur les partitions non croisées d’un cycle, *Discrete Mathematics* **1**, 333 (1972).

[22] R. Simion, Noncrossing partitions, *Discrete Mathematics* **217**, 367 (2000).

[23] A. Strominger and C. Vafa, Microscopic origin of the Bekenstein-Hawking entropy, *Physics Letters B* **379**, 99 (1996), arXiv:hep-th/9601029 [hep-th].

[24] G. Penington, Entanglement wedge reconstruction and the information paradox, *Journal of High Energy Physics* **2020**, 2 (2020), arXiv:1905.08255 [hep-th].

[25] A. Almheiri, N. Engelhardt, D. Marolf, and H. Maxfield, The entropy of bulk quantum fields and the entanglement wedge of an evaporating black hole, *Journal of High Energy Physics* **2019**, 63 (2019), arXiv:1905.08762 [hep-th].

[26] C. Akers and P. Rath, Holographic Renyi entropy from quantum error correction, *Journal of High Energy Physics* **2019**, 52 (2019), arXiv:1811.05171 [hep-th].

[27] X. Dong, D. Harlow, and D. Marolf, Flat entanglement spectra in fixed-area states of quantum gravity, *Journal of High Energy Physics* **2019**, 240 (2019), arXiv:1811.05382 [hep-th].

[28] X. Dong and D. Marolf, One-loop universality of holographic codes, *Journal of High Energy Physics* **2020**, 191 (2020), arXiv:1910.06329 [hep-th].

[29] D. Marolf, S. Wang, and Z. Wang, Probing phase transitions of holographic entanglement entropy with fixed area states, *Journal of High Energy Physics* **2020**, 84 (2020), arXiv:2006.10089 [hep-th].

[30] X. Dong and H. Wang, Enhanced corrections near holographic entanglement transitions: a chaotic case study, *Journal of High Energy Physics* **2020**, 7 (2020),

arXiv:2006.10051 [hep-th].

[31] C. Akers and G. Penington, Leading order corrections to the quantum extremal surface prescription, arXiv e-prints , arXiv:2008.03319 (2020), arXiv:2008.03319 [hep-th].

[32] G. Penington, S. H. Shenker, D. Stanford, and Z. Yang, Replica wormholes and the black hole interior, arXiv e-prints , arXiv:1911.11977 (2019), arXiv:1911.11977 [hep-th].

[33] S. Ryu and T. Takayanagi, Holographic Derivation of Entanglement Entropy from the anti de Sitter Space/Conformal Field Theory Correspondence, *Phys. Rev. Lett.* **96**, 181602 (2006), arXiv:hep-th/0603001 [hep-th].

[34] A. Dymarsky, N. Lashkari, and H. Liu, Subsystem eigenstate thermalization hypothesis, *Phys. Rev. E* **97**, 012140 (2018), arXiv:1611.08764 [cond-mat.stat-mech].

[35] R. Caginalp, M. Moosa, and P. Rath, Private Communication.

[36] M. C. Bañuls, J. I. Cirac, and M. B. Hastings, Strong and Weak Thermalization of Infinite Nonintegrable Quantum Systems, *Phys. Rev. Lett.* **106**, 050405 (2011), arXiv:1007.3957 [quant-ph].

[37] A. Kitaev, A simple model of quantum holography (2015), KITP Program: Entanglement in Strongly-Correlated Quantum Matter.

SUPPLEMENTAL MATERIAL

I. CHAOTIC EIGENSTATES

We provide a numerical study of relative entropy between mid-spectrum eigenstates of integrable and chaotic spin chains of length N with Hamiltonian

$$H = - \sum_{i=1}^N (Z_i Z_{i+1} + h_x X_i + h_z Z_i), \quad (29)$$

where X and Z are Pauli spin operators. We take $h_x = 1$, $h_z = 0$ for the integrable limit and $h_x = -1.05$, $h_z = 0.5$ for the chaotic regime as in Ref. [36]. We also numerically study the Sachdev-Ye-Kitaev model [37] with Hamiltonian

$$H = \sum_{j < k < l < m}^N J_{ijkl} \chi_j \chi_k \chi_l \chi_m, \quad \overline{J_{ijkl}^2} = \frac{6}{(N-3)(N-2)(N-1)} J^2, \quad (30)$$

where the χ_i 's are Majorana fermions and J_{ijkl} is a Gaussian random variable. The comparison between numerical data and (23) from the main text is shown in Fig. S1. The eigenstates are chosen randomly from the middle of the spectrum. The SYK model matches very well with (23). This may be expected because the Hamiltonian is a random matrix and the SYK model is known to be closely related to low-dimensional gravitational systems. The chaotic spin chain eigenstates have relative entropy close to, but noticeably larger than, random mixed states. This is reasonable because these eigenstates are not truly random and therefore should be more easily distinguishable. It would be interesting to understand whether this is a finite size bug or a feature that holds in the thermodynamic limit. Meanwhile, the integrable eigenstates are even more distinguishable, which is consistent with their violation of the eigenstate thermalization hypothesis. Moreover, the variance in relative entropy from eigenstate to eigenstate is much larger for the integrable spin chain.

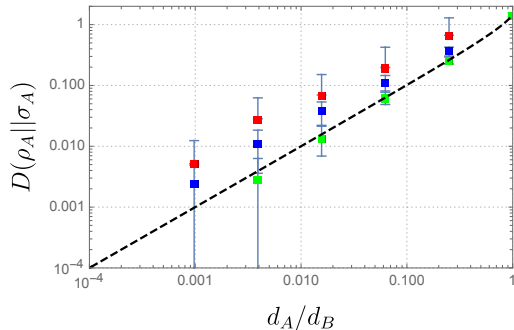


FIG. S1. The relative entropy between 10^3 random pairs of mid-spectrum eigenstates. The blue (red) data points are for the chaotic (integrable) spin chain with 12 spins and the dashed line is (23) from the main text. The green data points are for the SYK model with 20 Majorana fermions. We have omitted the lower error bars for the red data points for clarity, as they are very large and get in the way of the other data.